Catalystlike role of impurities in speeding layer-by-layer growth

Tien M. Phan [1], Stephen Whitelam,[2,*] and Jeremy D. Schmit[1,†]

[1]*Department of Physics, Kansas State University, Manhattan, Kansas 66506, USA*
[2]*Molecular Foundry, Lawrence Berkeley National Laboratory, 1 Cyclotron Road, Berkeley, California 94720, USA*

Molecular self-assembly is usually done at low supersaturation, leading to low rates of growth, in order to allow time for binding mistakes to anneal. However, such conditions can lead to prohibitively long assembly times where growth proceeds by the slow nucleation of successive layers. Here we use a lattice model of molecular self-assembly to show that growth in this regime can be sped up by impurities, which lower the free-energy cost of layer nucleation. Under certain conditions impurities behave almost as a catalyst in that they are present at high concentration at the surface of the assembling structure, but at low concentration in the bulk of the assembled structure. Extrapolation of our numerics using simple analytic arguments suggests that this mechanism can reduce growth times by orders of magnitude in parameter regimes applicable to molecular systems.

I. INTRODUCTION

The difficulty of achieving reliable self-assembly is one of controlling time scales [1–5]. While it is relatively easy to design a system in which the desired product is the thermodynamic ground state, it is more difficult to ensure that relaxation to equilibrium happens on observable time scales. If a structure grows more rapidly than its component pieces can sample their positional and conformational degrees of freedom then these components become trapped in nonoptimal states. This is the case for simple components, such as colloids, and complex components, such as biomolecules [6–9]. It is useful to arrange for the free-energy difference between the desired structure and the starting solution to be small, so that structures grow slowly enough that their constituent particles have time to relax to their preferred configurations [10–17]. A small free-energy difference can be achieved under conditions of small supercooling or low supersaturation. However, while such conditions help to avoid trapped states composed of improperly bound molecules, they exacerbate another kinetic trap, the long induction time associated with nucleation [18–21]. This kinetic trap can also impair growth when growth occurs in a layer-by-layer fashion, because nucleation is the rate-determining step for each stage of growth.

In this paper we use computer simulations of growing three-dimensional (3D) lattice-based structures to show that impurity particles can dramatically speed up layer-by-layer growth at low supersaturation, with little effect on the purity of the grown structure. Impurities are generally regarded as problematic, because they have the potential to arrest growth by "poisoning" the growth front [22,23]. However, we find that impurities can *speed* nucleation in the layer-by-layer growth regime, by lowering the free-energy cost of 2D layer nuclei and providing extra nucleation sites [24,25]. Impurities appear in the final 3D structure in low concentration, and in this respect behave almost as a catalyst.

Simple scaling results explain this catalystlike mechanism, and suggest that it should be relevant to a wide range of molecular and nanoscale systems. Let $\Delta\epsilon$ be the energy difference between a particle-particle bond and a particle-impurity bond, and let z_b and $z_s \approx z_b/2$ be the bulk and surface coordination numbers of the structure. If the time intervals between successive nucleation events are long, then a fraction $f_s \approx \exp(-\beta z_s \Delta\epsilon)$ of surface particles will be impurities [here $\beta \equiv 1/(k_B T)$]. Impurities can be numerous enough to lower the barrier to 2D nucleation, and therefore substantially increase the layer-by-layer growth rate, which scales as the exponential of this barrier. Impurities near the growth front can exchange with solution before the front moves away, leading to a bulk impurity fraction $f_b \approx \exp(-\beta z_b \Delta\epsilon) < f_s$. For large $\beta\Delta\epsilon$ this effect is akin to that of a catalyst, in that impurities can be abundant at the growth front, substantially increase the growth rate, and yet reside in the final structure in much smaller number. This speedup of growth is reminiscent of the nucleation enhancement of colloidal clusters by liquid-vapor critical fluctuations [26], in the sense that impurities serve as a source of fluctuations that promote a desired ordering process.

II. MODEL

We demonstrate this effect using a lattice model of two-component growth introduced previously [27,28]. Lattice sites can be vacant (white), or occupied by blue or red particles; these represent crystal and impurity particles, respectively. We refer to a blue structure as a crystal. Contacts between nearest-neighbor blue particles contribute a favorable binding energy $-\epsilon_b < 0$, while blue-red and red-red contacts contribute a less favorable energy $-\epsilon_r < 0$ ($\epsilon_b > \epsilon_r$). White sites carry
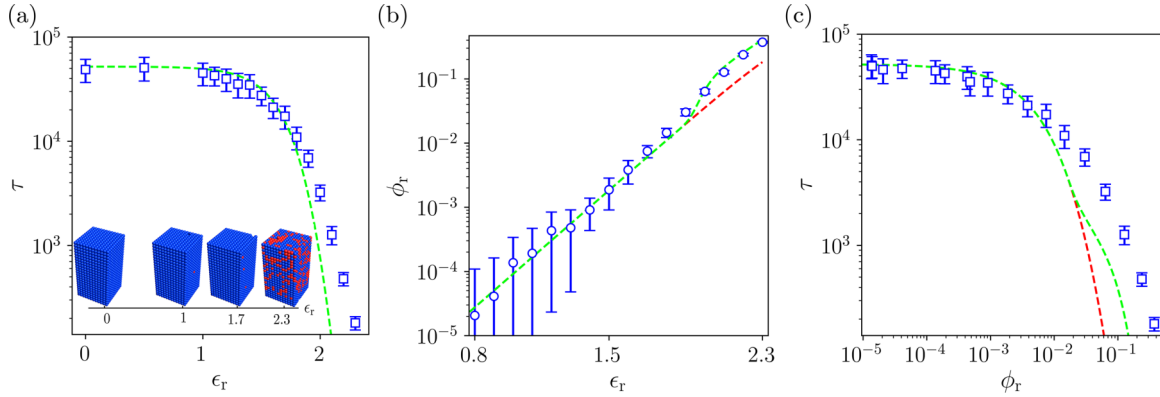
─────────────
*swhitelam@lbl.gov
†schmit@phys.ksu.edu

FIG. 1. (a) Layer addition time and representative snapshots and (b) impurity fraction for $\epsilon_b = 2.55$, $\Delta\mu = 0.25$. The dashed line in (a) is the prediction of Eq. (1), and the dashed lines in (b) and (c) are the predictions of Eq. (10) (red) and Eq. (11) (green). For impurity binding energies $\epsilon_r < 1.9$ ($\phi_r < 10^{-2}$) impurity relaxation is sufficiently fast that the solid composition can be approximated by the equilibrium result (red), whereas for large binding energies additional impurities become trapped by the advancing growth front (green). (c) Parametric plot of the data in panels (a) and (b) showing the layer addition time as a function of impurity fraction.

an energy penalty of μ. The quantity $\Delta\mu \equiv 3\epsilon_b - \mu$, which we call the supersaturation, is the bulk free-energy difference between an all-white state and an all-blue state; when $\Delta\mu > 0$ there exists a thermodynamic driving force to grow a crystal from solution. We carried out Monte Carlo simulations of this model on a 3D cubic lattice of 12×12 sites in the xy plane. Periodic boundary conditions were applied in this plane, and the crystal was seeded with three blue layers. The other direction, z, is the growth direction.

We evolved the model using the discrete-time Monte Carlo dynamics considered previously [27,28] (reproduced for completeness in the Appendix). To allow access to long time scales we carried out an additional set of simulations in which we imposed a solid-on-solid (SOS) restriction [29,30]: for sites with given values of (x, y) we proposed Monte Carlo moves only at two sites, the occupied site with the largest value of z and its neighboring unoccupied site. This restriction reduces the number of moves required to observe growth by a factor of order the length of the system (see the Appendix). It also artificially prevents vacancies within the solid, leading to a restricted equilibrium in which bulk vacancies do not exist [31]. However, in the regime studied here the equilibrium vacancy concentration is very small [32] and, as a result, the differences between our results in the presence and absence of the SOS constraint are negligible (see the Appendix). Here we present results obtained with the constraint.

III. IMPURITIES SPEED GROWTH

In Fig. 1 we show the mean time to grow one layer of the crystal, and the impurity fraction in the bulk, for various values of the impurity interaction ϵ_r (the impurity-free case corresponds to the limit $\epsilon_r \to -\infty$). Simulations were stopped when 20 layers were deposited [we define a layer as an (x, y) plane in which at least half the sites are occupied by colored particles]. The growth time is defined as the average number of Monte Carlo moves required to complete a layer. The impurity fraction is defined as the number of red particles divided by the number of colored particles. We see

that the growth time (eventually) decreases as the impurity binding energy increases, and the grown structure contains an increasing number of impurities. As we shall show, by varying conditions it is possible to have the growth time decrease more rapidly than the impurity fraction increases.

To estimate the growth time of the crystal we focus our discussion on the layer-by-layer growth regime at low temperature, where growth is limited by the nucleation of new layers on the crystal surface. When the time for 2D nucleation is much longer than the time for the resulting postcritical cluster to grow to completion, the layer growth time τ scales as

$$\tau \sim \exp(G_{\max}), \tag{1}$$

where $G_{\max}$ is the free energy of the critical 2D cluster (here and subsequently we work in units such that $k_B T = 1$). Equation (1) is valid when the layer completion time is short compared to the nucleation time, the regime on which we focus (more generally, see [29]). To estimate $G_{\max}$ we consider a $k \times k$ cluster on a flat blue surface [33]. Each particle incurs a chemical potential cost μ, so the chemical potential cost of the cluster is $k^2\mu = 3\epsilon_b k^2 - k^2\Delta\mu$. Each of the k^2 particles in the cluster makes one bond with the layer below it, and there are $2k(k-1)$ in-plane bonds. Thus the total bonding energy is $(-\epsilon_b) \times (3k^2 - 2k)$. Adding to this the chemical potential cost gives the energy cost for making a $k \times k$ square:

$$G(k) = 2k\epsilon_b - k^2\Delta\mu. \tag{2}$$

For nonzero supersaturation this function has a maximum at $k_\star = \epsilon_b/\Delta\mu$. The critical cluster therefore contains $k_\star^2 = (\epsilon_b/\Delta\mu)^2$ particles, and the corresponding energy barrier is $G(k_\star) = \epsilon_b^2/\Delta\mu$.

To understand how this result changes in the presence of impurities (red particles), consider the following simple argument. Let a lattice site be surrounded by z blue particles and $6 - z$ white particles, and let p be the probability that an isolated particle is a crystalline one as opposed to being an impurity (in simulations we model an equimolar mixture of crystal and impurity particles, and so set $p = 1/2$). At that lattice site, in a mean-field approximation, the thermal weight
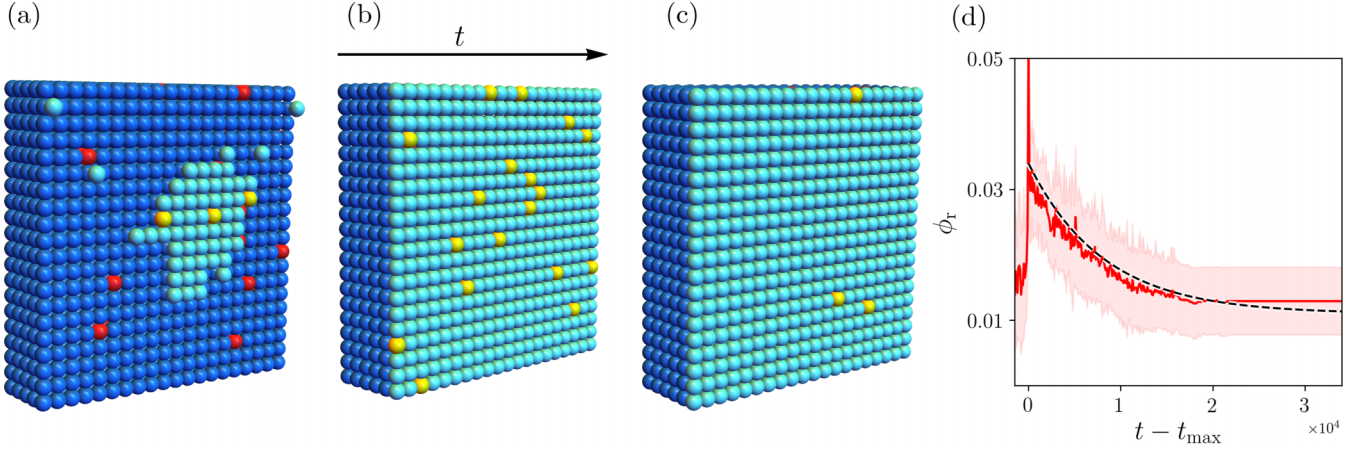
FIG. 2. Impurities are incorporated in each layer and gradually anneal to a more ordered structure. Snapshots of the annealing of a representative layer (in that layer only, blue particles are colored light blue, and red particles are colored yellow) (a) shortly after nucleation, (b) upon completion of the layer, and (c) after the growth front has moved away. Subsequent layers have been omitted for clarity. (d) Time progression of the impurity content in a layer (averaged over ten simulations). The decay of the impurity fraction after reaching a peak value (at $t = t_{\max}$) approaches the estimate Eq. (11) (dashed line).

of a red particle is $(1 - p)e^{z\epsilon_r}$, the thermal weight of a blue particle is $pe^{z\epsilon_b}$, and the thermal weight of a vacancy is e^μ. Thus the equilibrium fraction of colored particles is

$$f_1 = \frac{(1 - p)e^{z\epsilon_r} + pe^{z\epsilon_b}}{(1 - p)e^{z\epsilon_r} + pe^{z\epsilon_b} + e^\mu} = \frac{\mathcal{G}pe^{z\epsilon_b}}{\mathcal{G}pe^{z\epsilon_b} + e^\mu}, \quad (3)$$

where $\mathcal{G} \equiv 1 + (p^{-1} - 1)e^{-z\Delta\epsilon}$ and $\Delta\epsilon \equiv \epsilon_b - \epsilon_r$. The corresponding expression in the absence of impurities is

$$f_2 = \frac{pe^{z\epsilon_b}}{pe^{z\epsilon_b} + e^\mu}. \quad (4)$$

Comparison of f_1 and f_2 indicates that $\mathcal{G}$ functions as an effective degeneracy for blue particles. Alternatively, we can consider that the effective blue-particle interaction energy in the presence of impurities is larger than in their absence, i.e., $e^{z\epsilon_{\mathrm{eff}}} = \mathcal{G}e^{z\epsilon_b}$, giving

$$\epsilon_{\mathrm{eff}} = \epsilon_b + \frac{1}{z}\ln[1 + (p^{-1} - 1)e^{-z\Delta\epsilon}]. \quad (5)$$

The argument leading to (2) can now be modified, by replacement of ϵ_b with ϵ_{eff} in the bond-energy reward term, to estimate the energy cost $G_{\mathrm{eff}}(k) = G(k) + \Delta G(k)$ required to make a $k \times k$ cluster in a solution of particles and impurities:

$$\Delta G(k) = \frac{k(2 - 3k)}{z}\ln[1 + (p^{-1} - 1)e^{-z\Delta\epsilon}]. \quad (6)$$

To estimate the mean coordination number z as a function of k, note that in a $k \times k$ cluster we have $(k - 2)^2$ particles with four in-plane bonds, $4(k - 2)$ particles with three in-plane bonds, and four corner particles with two in-plane bonds. Each particle makes one extra bond with the substrate. Thus the average coordination number is $z(k) = 5 - 4/k$. Inserting $z(k)$ into (6) gives

$$\Delta G(k) = -\frac{k^2(3k - 2)}{5k - 4}\ln[1 + (p^{-1} - 1)e^{-\Delta\epsilon(5 - 4/k)}]. \quad (7)$$

The right-hand side of (7) describes the impurity-induced reduction in the energy cost of a $k \times k$ cluster (we recover the no-impurity case in the limit $\Delta\epsilon \to \infty$). For small $\Delta\mu$ the function $G_{\mathrm{eff}}(k)$ will take its maximum at a value of $k \gg 1$. In this regime we can expand (7) to get $G_{\mathrm{eff}}(k) \approx 2k\epsilon_b - k^2\mu_{\mathrm{eff}}$, which has the same form as the impurity-free expression (2) but with effective supersaturation,

$$\Delta\mu_{\mathrm{eff}} = \Delta\mu + \tfrac{3}{5}\ln[1 + (p^{-1} - 1)e^{-5\Delta\epsilon}]. \quad (8)$$

The free-energy barrier to layer nucleation in the presence of impurities can then be estimated as

$$G_{\max} \approx \frac{\epsilon_b^2}{\Delta\mu_{\mathrm{eff}}}. \quad (9)$$

Note that the reduction to the nucleus free energy enters through the bulk term, not the surface term as is typical in models of heterogeneous nucleation at a surface.

We next consider the fraction of impurities involved during growth (in the parameter regime in which this fraction is small). For a lattice site surrounded by z blue particles, the equilibrium fraction of red particles is

$$\phi(z) = \frac{(1 - p)e^{z\epsilon_r}}{(1 - p)e^{z\epsilon_r} + pe^{z\epsilon_b}} = \frac{1 - p}{1 - p + p\,e^{z\Delta\epsilon}}. \quad (10)$$

This fraction is smaller in the interior of the crystal, where the impurity makes $z_b = 6$ blue contacts, than at the surface.

As the completed layer becomes covered by new particles, it will evolve toward the bulk defect concentration. The time scale for this relaxation, τ_r, is the time scale for a fivefold-coordinated particle at the surface to unbind, and so we estimate $\tau_r \propto e^{5\epsilon_r}$. Provided the layer addition time τ is longer than this, we estimate the impurity fraction in a newly completed layer as

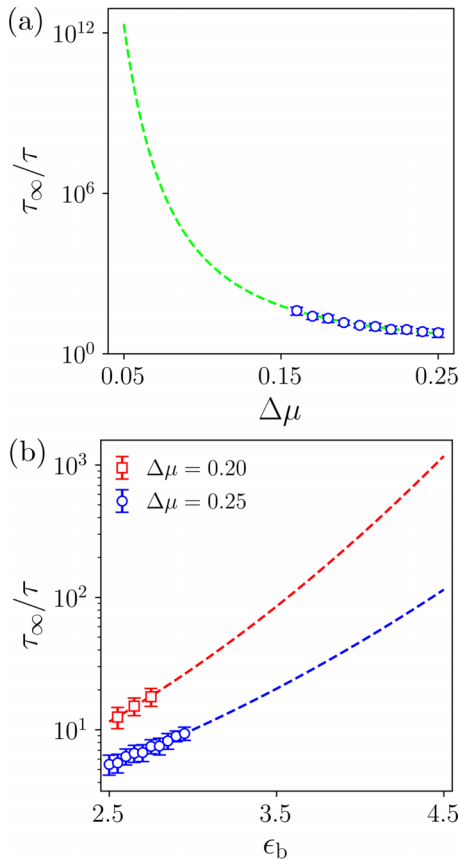$$\phi_r \approx \phi(5)e^{-\tau/\tau_r} + \phi(6). \quad (11)$$

FIG. 3. Ratio of the growth time τ in the presence of impurities to that in the impurity-free case, τ_∞, as a function of (a) supersaturation and (b) binding energy. The beneficial effect of impurities is most pronounced in the presence of small supersaturation and large binding energies. In both panels, parameters are chosen so that the bulk equilibrium impurity fraction is always 1%. The dashed lines are the predictions of Eq. (1).

This annealing process is illustrated in Fig. 2. The snapshots (a)–(c) and time-trace (d) show that impurity particles are present at higher concentration at the growth front than in the bulk of the structure. The relaxation of the impurity fraction from the surface to the bulk equilibrium concentration occurs in a manner consistent with (11); see panel (d).

IV. IDENTIFYING THE PARAMETER REGIME IN WHICH IMPURITIES ARE OF MOST BENEFIT

The preceding analysis confirms that impurities speed layer nucleation, via (1), (8), and (9), and make the equilibrium solid less pure, via (10). Impurities are most beneficial when the former effect is as large as possible, and the latter effect as small as possible. To make the bulk equilibrium impurity concentration (10) small we want $\Delta\epsilon$ large; we then want $\Delta\mu$ small, so that the second term in (8) remains significant.

In Fig. 3 we show that these predictions are consistent with our simulations: a crystal of a certain impurity fraction

grows more rapidly than its impurity-free counterpart, and this effect is much enhanced as supersaturation is reduced. Our predictions also suggest that impurities can be orders of magnitude more effective in parameter regimes that are inaccessible to our simulations but which describe molecular systems.

V. CONCLUSIONS

Impurities are often considered to be problematic when attempting to grow crystals, but we have shown that layer-by-layer growth can be dramatically sped up by impurities with little impact on the quality of the final structure. Our computer simulations and simple scaling arguments suggest that this effect will be most pronounced under conditions of low supersaturation and low temperature. Such conditions are often required for the crystallization of highly anisotropic molecules, for which the probability of crystalline (or productive) binding is small. For example, proteins must sample an ensemble of $\simeq 10^4$–10^5 states in order to find the crystallographic state [34–36]. Given many ways of misbinding, growth must be slow (and so supersaturation must be low) in order to allow time for error correction. Furthermore, a large binding energy is needed to offset the entropic advantage of the disordered ensemble [37]. This combination of large binding energies and low supersaturation leads to high surface tension and long nucleation times, precisely the region in which impurities are expected to be beneficial [Fig. 3(b)]. Indeed, this mechanism may provide an explanation for the utility of nonspecific binding enhancers in protein crystallization [38–40], such as depletants, in the layer-by-layer growth regime.

APPENDIX: LATTICE MODEL MONTE CARLO DYNAMICS

The unrestricted Monte Carlo protocol proceeds as follows. At each step of the simulation a site was chosen at random. If the chosen site was white then we proposed with probability p (respectively $1 - p$) to make it blue (respectively red). If

the chosen site was red or blue then we proposed to make it white. No red-blue interchange was allowed. These proposals were accepted with probabilities

$$R \rightarrow W : \min(1, (1 - p) \exp(-\Delta E));$$
$$W \rightarrow R : \min(1, (1 - p)^{-1} \exp(-\Delta E));$$
$$B \rightarrow W : \min(1, p \exp(-\Delta E));$$
$$W \rightarrow B : \min(1, p^{-1} \exp(-\Delta E)), \tag{A1}$$

where ΔE is the energy change resulting from the proposed move. This change was calculated from the lattice energy function

$$E = \sum_{\langle i,j \rangle} \epsilon_{C(i)C(j)} + \sum_i \mu_{C(i)}. \tag{A2}$$

The first sum runs over all distinct nearest-neighbor interactions. The second sum runs over all sites. The index $C(i)$ describes the color of site i and is W (white), B (blue), or R (red); $\epsilon_{C(i)C(j)}$ is the interaction energy between colors $C(i)$ and $C(j)$ (this is zero if either site is white); and the chemical potential $\mu_{C(i)}$ is μ, $\ln p$ and $\ln(1 - p)$ for W, B, and R, respectively. In the main text we set $p = 1/2$ in order to model an equimolar mixture of crystal and impurity particles.

In the main text we describe a solid-on-solid (SOS) restricted protocol in which Monte Carlo moves are performed only at the growth front. This protocol, which does not allow vacancies to become incorporated into the 3D structure, results in a different equilibrium than the unrestricted protocol. However, in the parameter regime we probe the difference is slight, because few vacancies appear in the unrestricted protocol (Fig. 4), and the presence or absence of the restriction does not qualitatively affect our conclusions.
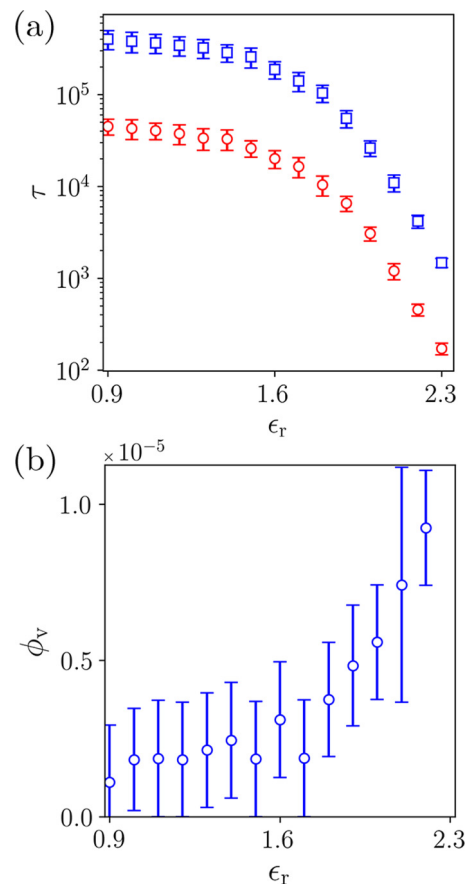

FIG. 4. The growth time (a) and average fraction of vacancies (b) in the bulk as a function of impurity binding energy. In (a), the SOS restriction (red) reduces the number of moves required to observe growth (by a factor of order the length of the system) compared with the unrestricted Metropolis Monte Carlo simulation (blue). (b) Fraction of vacancies in the bulk, averaged over 100 simulations, in the absence of the SOS restriction. These small vacancy fractions show that the effect of imposing the SOS restriction (which eliminates vacancies) is slight.

[1] S. Zhang, Nat. Biotechnolnol. **21**, 1171 (2003).
[2] J. C. Huie, Smart Mater. Struct. **12**, 264 (2003).
[3] B. A. Lindquist, R. B. Jadrich, and T. M. Truskett, J. Chem. Phys. **145**, 111101 (2016).
[4] S. Whitelam and R. L. Jack, Annu. Rev. Phys. Chem. **66**, 143 (2015).
[5] A. W. Long and A. L. Ferguson, Mol. Syst. Des. Eng. **3**, 49 (2018).
[6] A. W. Wilber, J. P. Doye, A. A. Louis, E. G. Noya, M. A. Miller, and P. Wong, J. Chem. Phys. **127**, 085106 (2007).
[7] D. C. Rapaport, Phys. Rev. Lett. **101**, 186101 (2008).
[8] M. F. Hagan and D. Chandler, Biophys. J. **91**, 42 (2006).
[9] T. K. Haxton and S. Whitelam, Soft Matter **8**, 3558 (2012).
[10] K. Kremer, J. Aerosol Sci. **9**, 243 (1978).
[11] D. Stauffer, J. Aerosol Sci. **7**, 319 (1976).
[12] H. Trinkaus, Phys. Rev. B **27**, 7372 (1983).
[13] J. Schmelzer, A. Abyzov, and J. Möller, J. Chem. Phys. **121**, 6900 (2004).
[14] J. Schmelzer, J. Schmelzer Jr, and I. Gutzow, J. Chem. Phys. **112**, 3820 (2000).
[15] R. Scarlett, J. Crocker, and T. Sinno, J. Chem. Phys. **132**, 234705 (2010).
[16] A. Kim, R. Scarlett, P. Biancaniello, T. Sinno, and J. Crocker, Nat. Mater. **8**, 52 (2008).
[17] R. Scarlett, M. Ung, J. Crocker, and T. Sinno, Soft Matter **7**, 1912 (2011).
[18] N. M. Dixit and C. F. Zukoski, Phys. Rev. E **66**, 051602 (2002).
[19] S. A. Kulkarni, S. S. Kadam, H. Meekes, A. I. Stankiewicz, and J. H. ter Horst, Cryst. Growth Des. **13**, 2435 (2013).
[20] T. E. Paxton, A. Sambanis, and R. W. Rousseau, Langmuir **17**, 3076 (2001).
[21] J. K. Dhont, C. Smits, and H. N. Lekkerkerker, J. Colloid Interface Sci. **152**, 386 (1992).
[22] G. Ungar, E. G. R. Putra, D. S. M. de Silva, M. A. Shcherbina, and A. J. Waddon, Adv. Polym. Sci. **180**, 45 (2005).

[23] T. Schilling and D. Frenkel, J. Phys.: Condens. Matter **16**, S2029 (2004).

[24] M. van der Leeden, D. Kashchiev, and G. van Rosmalen, J. Cryst. Growth **130**, 221 (1993).

[25] R. M. Ginde and A. S. Myerson, J. Cryst. Growth **126**, 216 (1993).

[26] P. R. ten Wolde and D. Frenkel, Science **277**, 1975 (1997).

[27] S. Whitelam, R. Schulman, and L. Hedges, Phys. Rev. Lett. **109**, 265506 (2012).

[28] S. Whitelam, L. O. Hedges, and J. D. Schmit, Phys. Rev. Lett. **112**, 155504 (2014).

[29] Y. Saito, *Statistical Physics of Crystal Growth* (World Scientific, Singapore, 1996).

[30] J. M. Kim and J. M. Kosterlitz, Phys. Rev. Lett. **62**, 2289 (1989).

[31] This restriction also prevents nonphysical vacancy-catalyzed annealing in the interior of the solid [37].

[32] S. Whitelam, J. Chem. Phys. **149**, 104902 (2018).

[33] An accurate expression for 2D nuclei of irregular shape can be found in Ref. [41]; approximating nuclei as squares incurs numerical errors, but captures important trends of barrier height with model parameters.

[34] D. Asthagiri, A. Lenhoff, and D. Gallagher, J. Cryst. Growth **212**, 543 (2000).

[35] A. M. Kierzek, W. M. Wolf, and P. Zielenkiewicz, Biophys. J. **73**, 571 (1997).

[36] J. D. Schmit and K. Dill, J. Am. Chem. Soc. **134**, 3934 (2012).

[37] S. Whitelam, Y. R. Dahal, and J. D. Schmit, J. Chem. Phys. **144**, 064903 (2016).

[38] P. G. Vekilov and J. I. D. Alexander, Chem. Rev. **100**, 2061 (2000).

[39] R. Giegé, FEBS J. **280**, 6456 (2013).

[40] S. D. Durbin and G. Feher, Annu. Rev. Phys. Chem. **47**, 171 (1996).

[41] S. Ryu and W. Cai, Phys. Rev. E **81**, 030601(R) (2010).